

Numerical Weather Prediction activities at CHMI

R. Brožková, A. Bučánek, J. Mašek, D. Němec, A. Šljivić, P. Smolíková, A. Trojáková

NWP system

ALADIN/CHMI couples non-hydrostatic (NH) dynamics and the set of ALARO-1vB physical parameterizations suited for modeling of atmospheric motions from planetary up to the meso-gamma scales:

- domain 1069x853 grid points, $\Delta x \sim 2.3\text{km}$
- linear truncation E539x431
- 87 vertical levels, mean orography
- ICI scheme with 1 iteration, time step 90 s
- 3h coupling interval
- 00, 06, 12/18 UTC forecast to +72/54h
- hourly analysis system VarCan Pack
- ALADIN cycle 46t1mp (ALARO-1vB)

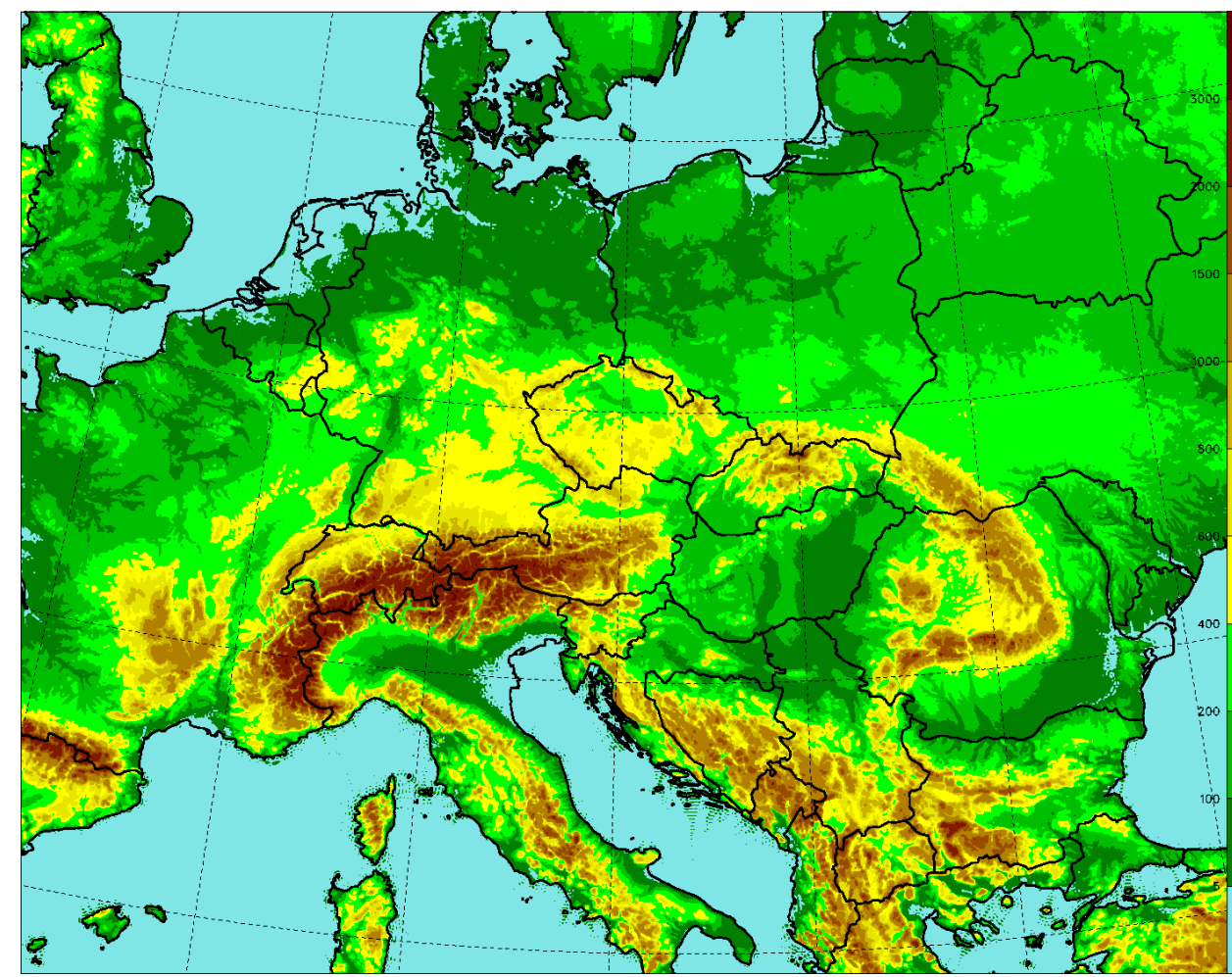


Fig. 1. Orography of the domain.

Data assimilation includes surface analysis based on an optimal interpolation (OI) and BlendVar analysis for upper air fields, which consists of the digital filter spectral blending (Brozkova et al., 2001) followed by the 3DVAR analysis (Fischer et al., 2005)

- digital filtering at truncation E102x81; space consistent coupling
- no DFI in long cut-off 3h cycle; incremental DFI in short cut-off production analysis
- observations: SYNOP, TEMP, AMDAR, Mode-S, SEVIRI, WP, HR-AMV, ASCAT

HPC systems

Two HPC systems at CHMI:

NEC SX Aurora TSUBASA

48 computing nodes with:

- one AMD EPYC 7402 CPU (24 cores, 512GB RAM), and
- eight NEC Vector Engines 20B (8 cores, 48GB RAM each)
- total 1152 VH + 3072 VE cores

NEC LX series HPC cluster

- 320 computing nodes with:
- Intel Broadwell CPU (2x12 cores, 64GB RAM)
- total 7680 computational cores



Fig. 2. NEC SX Aurora

Radar reflectivity

The size distribution of rain proposed by Abel and Boutle (2012) was implemented for radar reflectivity diagnostics, making it consistent with the size distribution used in the microphysics scheme. This distribution delivers smaller particles in the case of low mass fraction of rain and bigger in heavy rain than the formerly used Marshall-Palmer one. Thus, simulated reflectivities are lower in drizzle and light rain and higher in heavy precipitation.

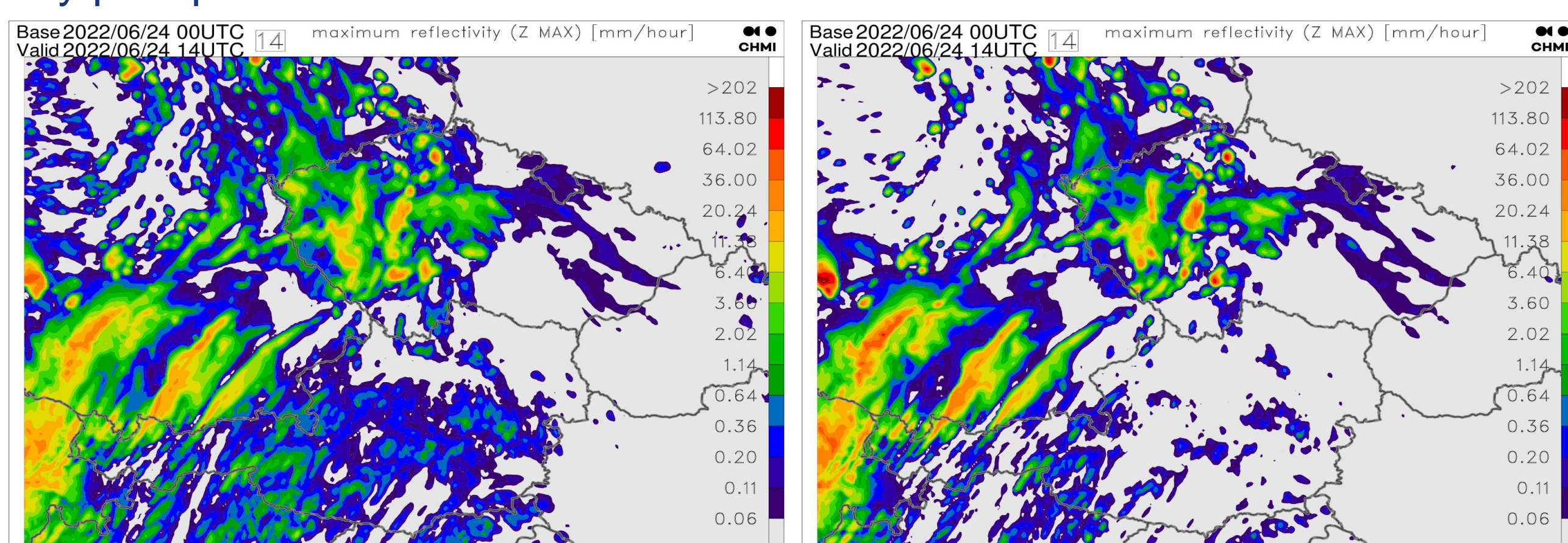


Fig. 3. Simulated maximum reflectivity with default (Marshall-Palmer) distribution of rain (left) and Abel and Boutle distribution (right) for 24 Jun 2022 00UTC +14h.

The data assimilation of radar reflectivity volumes from OPERA is currently under investigation in ALARO CMC. The 1D+3D-Var assimilation method (Wattrelot et al., 2014) is employed, which indirectly assimilates radar reflectivity as humidity profiles. Initial experiments demonstrated a significant systematic drying caused by "non-rainy" observations (undetected). A promising approach to mitigate excessive drying is a combination of error inflation for observations created from undetected pixels and the threshold method. The threshold method assimilates reflectivity observations only when the observed or modelled reflectivity exceeds a threshold, which is 0 DBZ in this case. The Abel and Boutle rain size distribution provides another opportunity to improve the radar observation operator.

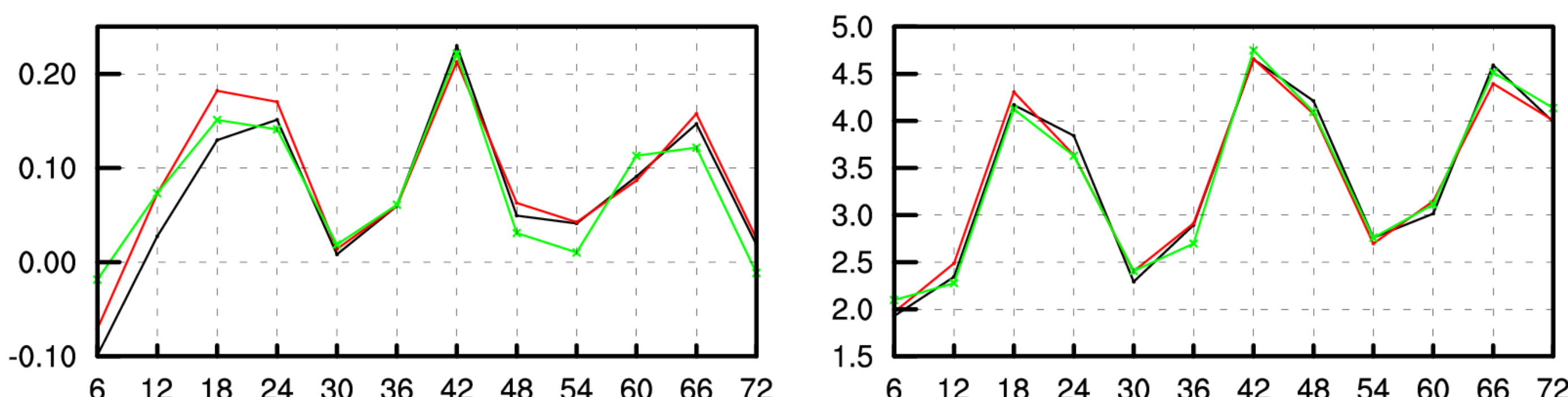


Fig. 4. Time evolution of BIAS (left) and RMSE (right) of 6h precipitation for period of 15 – 30 Jun 2024 00UTC. Reference (operational run), reflectivity assimilation and reflectivity assimilation using new size distribution in the observation operator.

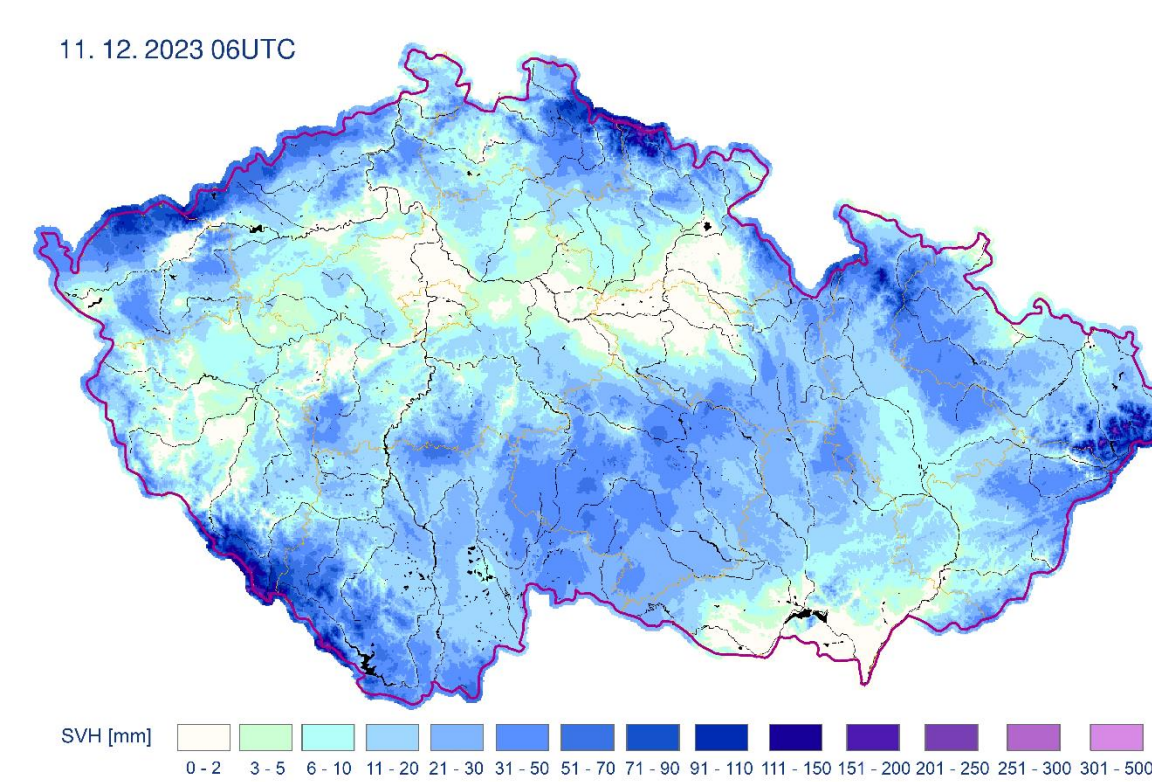
Major operational changes

6 Feb 2024

Increase of long cut-off assimilation frequency from 6h to 3h and the new setting of surface assimilation and snow roughness (see description below). The new Lopez evaporation parametrization and retuned autoconversions to snow and cloud water (presentation of David Němec). New wind gust diagnostic based on TKE at 20m.

New snow treatment

The original surface analysis setup included a weak relaxation to the climatology (RCLIMCA=0.045). We halved it (RCLIMCA=0.0225) when switching to a 3-hour cycle (complete removal of relaxation caused a bias of 2m temperature and a small daily amplitude). However, we left it off for snow to get more realistic amount of snow.



The snow water equivalent improved with suppressed relaxation to climatology.

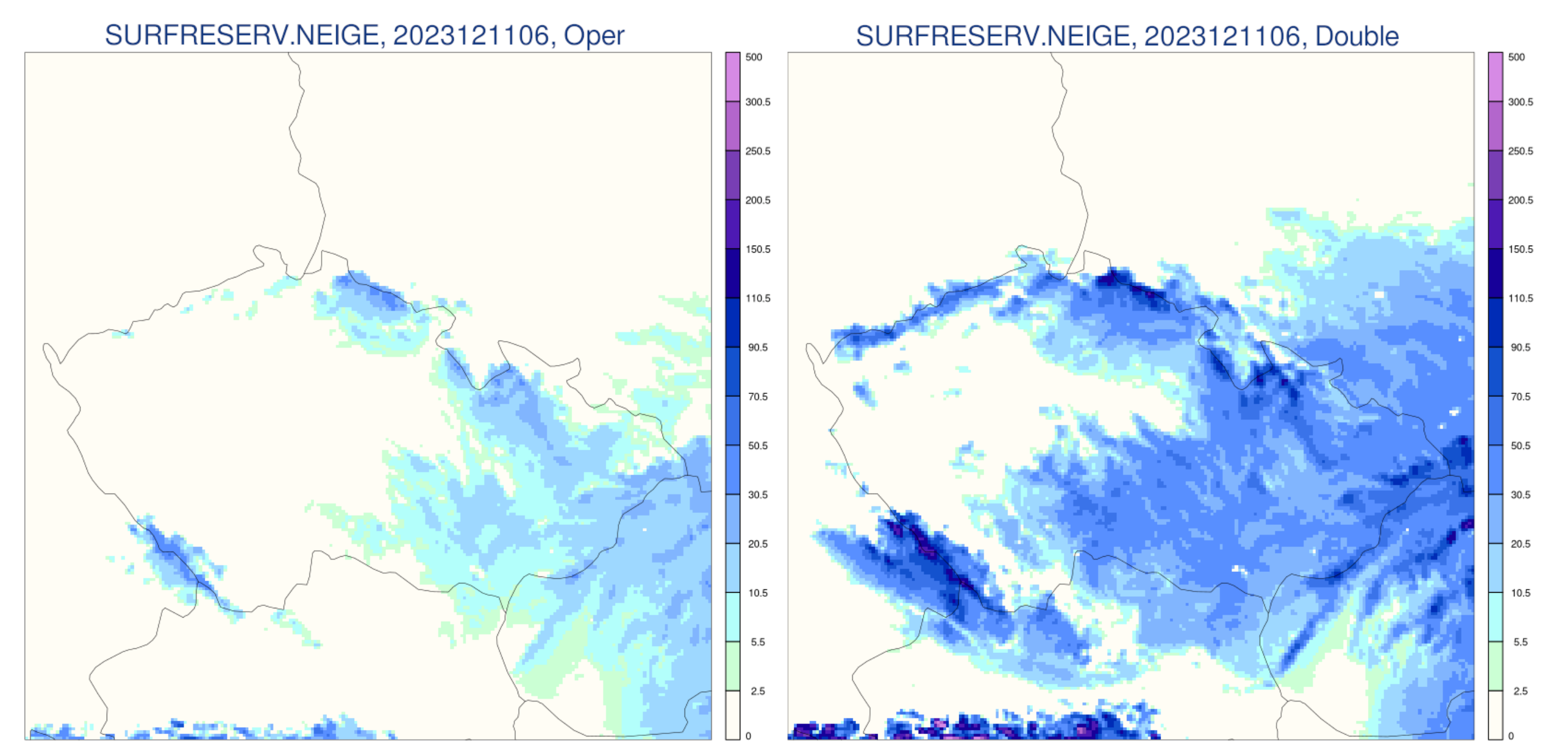
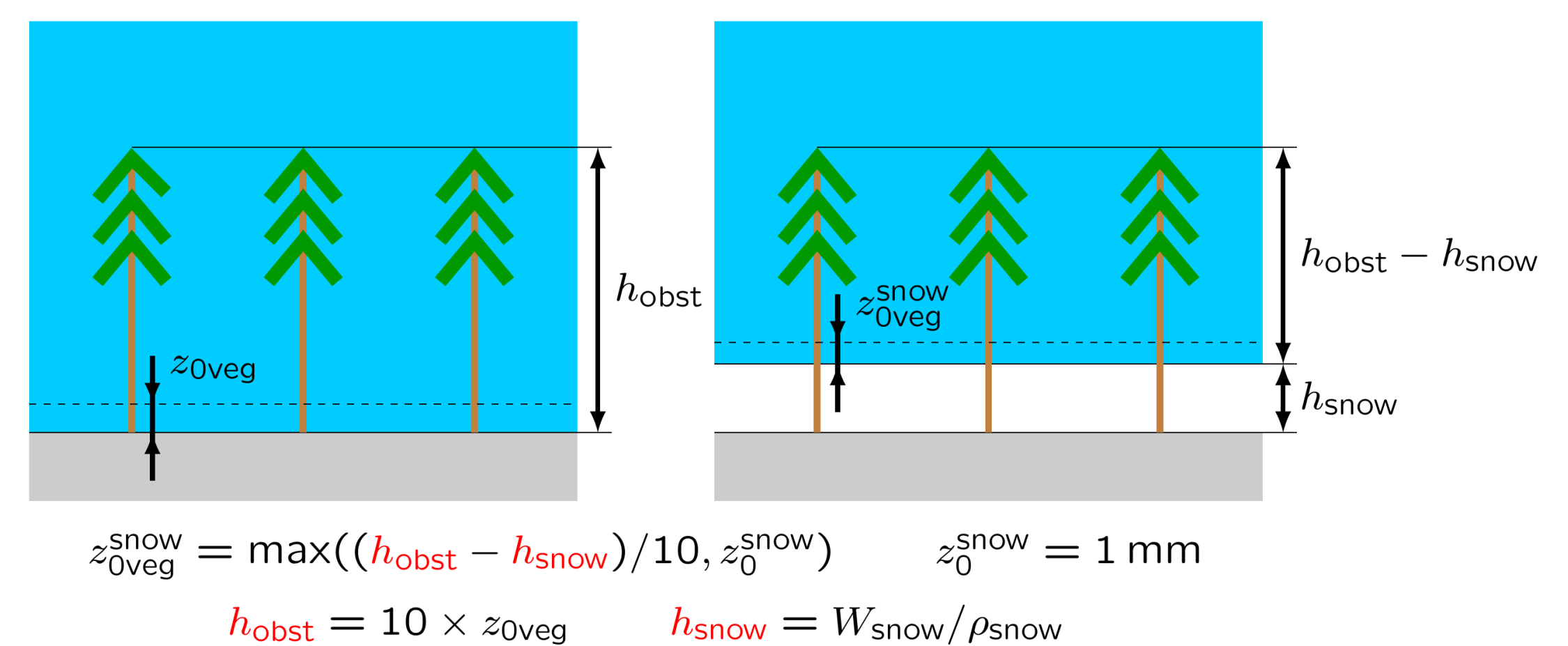


Fig. 5. Snow water equivalent (SWE) for 11 Dec 2023 06UTC, OPER (left) with a weak relaxation (RCLIMCA=0.045) and parallel test (right) with suppressed relaxation for snow (RCLIMSN=0) and the observation based estimate of SWE (top).

Larger amounts of snow needed adjustments to the roughness of the vegetation covered by snow (effect on wind speed) and its distribution within the grid-box (effect on temperature due to radiation).

The old treatment was averaging roughness lengths of vegetation and snow using snow fraction as weight. In case of large amount of snow over forest, it led to unrealistic reduction of roughness length, resulting in overestimated 10m wind speed. The new treatment employs approximate relation between mean obstacle height and roughness length, and it reduces the roughness length proportionally to the part of obstacle height covered by snow.



The new treatment (LZ0SNOWH=T, RZ0_TO_HEIGHT=0.1) was introduced (available since CY49T1) improving the bias of 10m wind speed (Figure 6). Cold bias of 2m temperature connected to higher amount of snow was reduced by retuning the snow fraction (parameter WCRIN is set to 10 instead of 4).

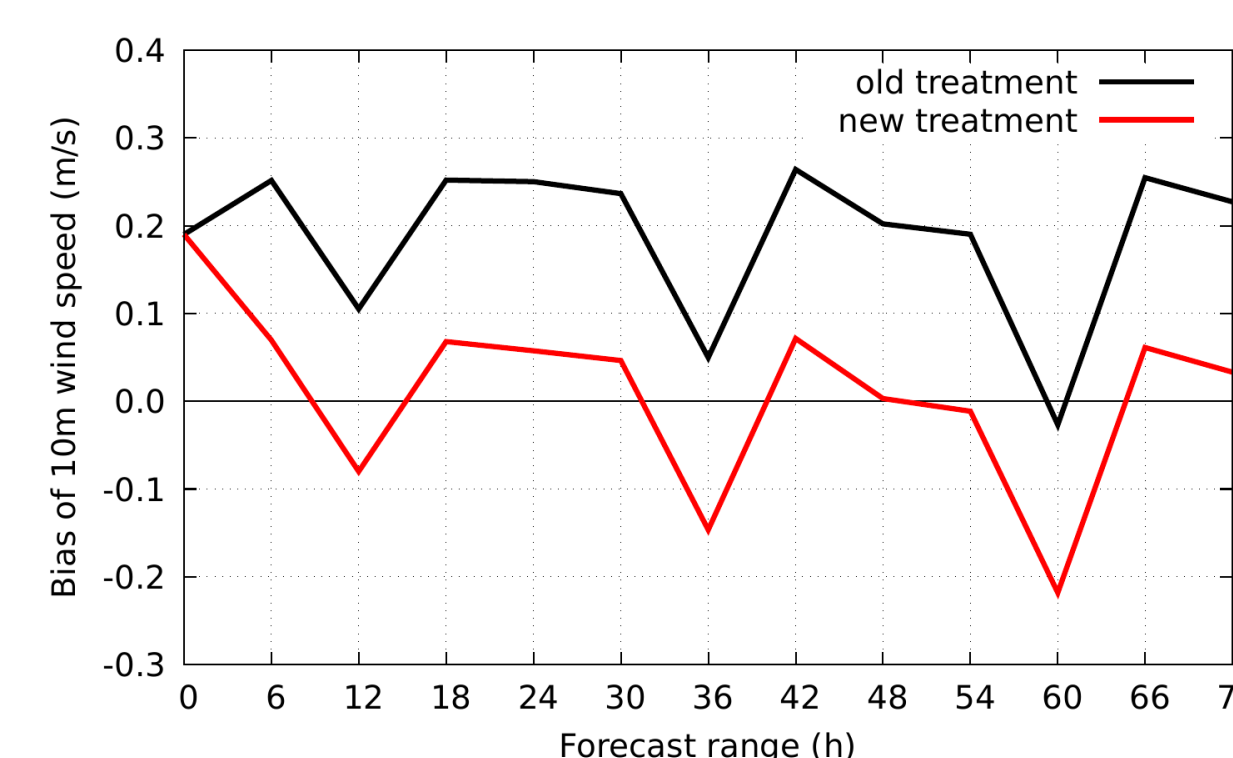


Fig. 6. Time evolution of BIAS of 10m wind speed for period of 1 – 8 Dec 2023 00UTC. Reference (old treatment) and new treatment of roughness lengths.

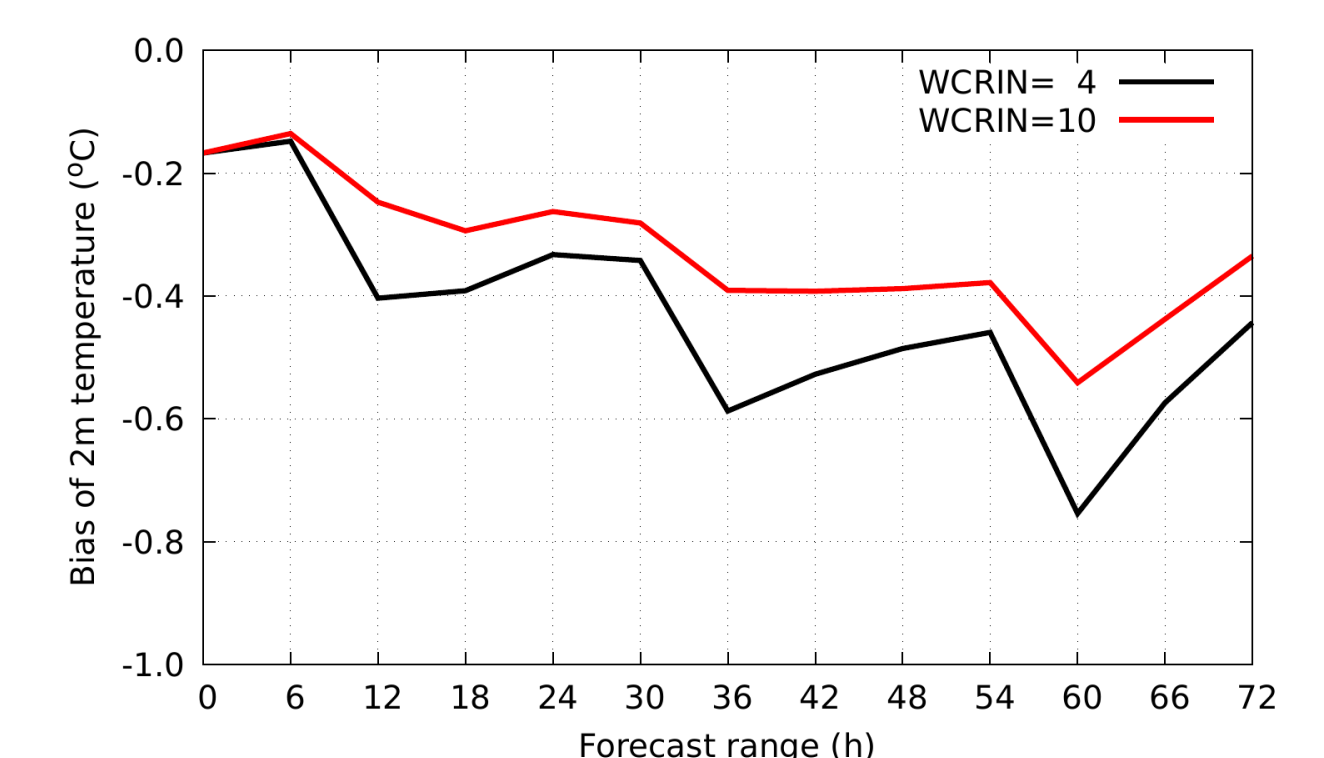


Fig. 7. Time evolution of BIAS of 2m temperature for period of 1 – 8 Dec 2023 00UTC. Reference (WCRIN=4) and new setting (WCRIN=10).